Wind Tunnel Tests on an Outer Wing Segment of the ASW-19X Sailplane

L.M.M. Boermans
B. Oolbekkink

Delft University of Technology
Department of Aerospace Engineering
The Netherlands

Presented at the 18th OSTIV Congress
Hobbs, New Mexico, June 28-July 9, 1983

INTRODUCTION

At the Delft University of Technology Low Speed Laboratory (LSL) an investigation was conducted to determine the aerodynamic characteristics of an outer wing segment of the ASW-19X sailplane. This sailplane is a Standard Class ASW-19B with a modified wing. New airfoils were designed such that just by adding material to the surface, the existing wing could be modified and tested in flight. Wind tunnel tests on an actual inner and outer wing segment of the original ASW-19B are described in Ref. 1, and a comprehensive paper on the considerations, tests and results of the ASW-19X research program - which led to an improvement of 5% in glide ratio over the entire practical flight speed range - is given in Ref. 2.

A special feature of the new wing is the application of pneumatic turbulators on the lower surface, a technique to reduce airfoil drag by avoiding pronounced laminar separation bubbles. Wind tunnel tests on the inner wing airfoil section showed a considerable drag decrease. At present, similar tests on an outer wing segment are described. In addition, tests with a tape with digged-in bumps instead of the pneumatic turbulators are described.

Wool tufts filmed by a camera mounted on a sting on top of the fuselage indicated flow separation on the downward deflected aileron in circling flight. In the present investigation attention was given to this phenomenon.

TEST SEGMENT

The left wing of the ASW-19X was suspended vertically such that a part of the outer wing passed through the test section of the wind tunnel, Fig. 1. The axis of rotation was parallel to the quarter chord line of the wing. Attachment took place by filling the gap between the wing and the turntables in the upper and lower tunnel wall with Araldite. The black line shown in Fig. 1 is a colored tape which covered

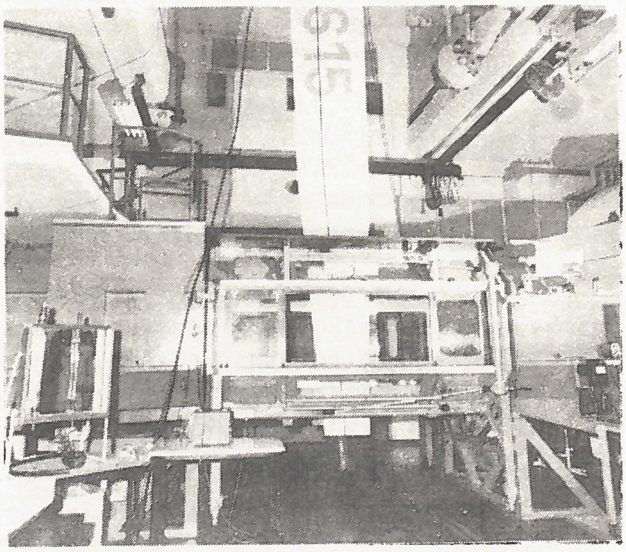

Fig. 1: Test set-up

the pneumatic turbulators (for testing purpose). These turbulators consist of 20 mm long tubes with 0.6 mm inner diameter and are installed with 16 mm interspace in a spanwise row. In flight, the air volume flow needed for the pneumatic turbulators is obtained in each wing half by means of a nozzle mounted on the streamline cap which covers the aileron actuator. The nozzle is located inside the wind tunnel test section as shown in Fig. 2. During the wind tunnel measurements the nozzle was closed with a streamlined plug and the volume flow for the pneumatic turbulators was obtained by pressurizing the wing to the internal wing pressure measured in flight. Fig. 2 also shows the location of the pneumatic turbulators and some other interspaces tested.

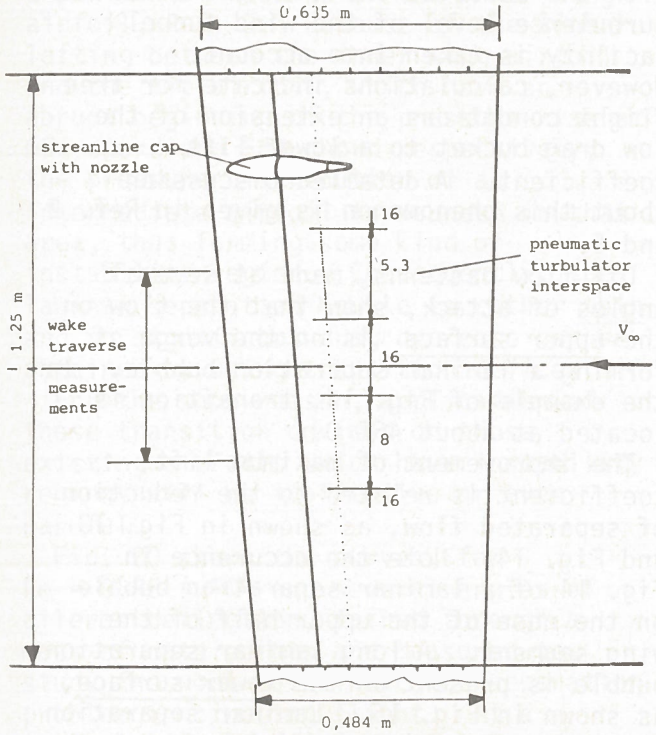

Fig. 2: Test segment and the turbulator interspaces tested.

From the root up to 59% semispan the wing is untwisted and has the airfoil DU80-176V1. From 59% semispan up to the tip the wing is linear lofted from DU80-176V1 to DU80-141, while a washout of 1.7 degrees is applied. Airfoil DU80-1767V1 is a slightly more cambered version of DU80-176 (DU 80-176: Delft University, 1980, thickness/chord ratio 0.176.), the latter airfoil was extensively tested at LSL. Fig. 3 and 4 show the airfoils fitted to the original airfoils and some potential flow pressure distributions. The upper surface aileron slot was sealed with the usual tape. The tape was flush with the wing surface (contrary to the ASW-19B where the tape was stuck on top of the surface).

WINDTUNNEL AND TEST EQUIPMENT

The wind tunnel used is the low-speed, low-turbulence wind tunnel of the Department of Aerospace Engineering at Delft University of Technology. The tunnel is of the closed return type and has an interchangeable octagonal test section of 1.80 m wide and 1.25 m high. The turbulence level in the test section varies from 0.018% at 10 m/s to 0.043% at 60 m/s.

Wall pressures were measured at 15 stations (equally spaced at 50 mm) in the plane of the mid-span section on each tunnel side wall. The position of these stations was symmetrical with respect to the quarter chord point of the model mid-span section.

A wake survey rake, mounted on a cross beam, was positioned with the tips of the total pressure tubes approximately a quarter chord length of the mid-span section downstream of the wing. The wake rake utilized 17 total pressure tubes equally spaced at 5 mm and 6 static pressure tubes. A pitot-static tube was mounted in the plane of the mid-span section on the tunnel wall opposite the lower surface of the wing.

All pressures were recorded by an automatically reading multi-tube liquid manometer (200 tubes).

The behavior of the airflow was investigated by means of an oilfilm technique and a stethoscope.

TESTS

Tests with zero aileron deflection were executed at practical combinations of angle of attack and Reynolds number and:

- with the pneumatic turbulators

inactive (sealed by tape of 0.04 mm thickness),

– with the pneumatic turbulators active. In addition to the usual 16 mm interspace of the pneumatic turbulators, some tests were performed with 8 mm and 5.3 mm interspace, Fig. 2,

– with a transition strip installed at the position of the pneumatic turbulators. The strip consists of self-sticking Mylar-film (width 11 mm, thickness 0.25 mm) with digged-in bumps. The height of the bumps is 1 mm and their interspace is 5 mm.

Tests with zero aileron deflection, active pneumatic turbulators, and the aileron slots smoothed with 0.04 mm thick tape, were executed in order to compare the results with the results of previous measurements on the original ASW-19B outer wing segment. This segment was built in the wing production mould especially for the wind tunnel tests and had, contrary to the actual wing, no aileron.

Tests with positive and negative aileron deflection were executed at a Reynolds number of $0.85 * 10^6$ which is relevant for low speed circling.

DATA REDUCTION

Test equipment and data reduction were similar to the original ASW-19B wing segment tests. The lift coefficient was obtained from the tunnel-wall pressures and the profile-drag coefficient was computed from the wake rate total and static pressures following the procedure described by Pfenninger, Ref. 3. For determining the free flight characteristics from the wind tunnel measurements the well-known correction method of Allen and Vincenti, Ref. 4, was applied. All data were on line reduced and the characteristics were plotted using the HP21MX-E computer of the laboratory.

RESULTS

The fairly uniform drag distribution measured at $\alpha = -2^o, 0^o$, and 7^o along 0.40 m span indicated that the quality of the wing segment was good. Fig. 5 shows for zero aileron deflection the characteristics with inactive pneumatic turbulators, and Fig. 6 with active pneumatic turbulators (interspace 16 mm). With the transition strip with bumps the characteristics of Fig. 7 are measured. A comparison of the results given in Fig. 8 show only minor drag differences. The explanation will be given below.

A drag reduction is obtained by smoothing the aileron slots with 0.04 mm thick tape, as shown in Fig. 9 and Fig. 10.

A comparison of the results with the previously measured characteristics of the original ASW-19B outer wing section, Fig 11, shows the drag reduction and increase in maximum lift coefficient obtained with the modification.

The measured lower end of the low drag bucket at $C_\ell \approx 0.2$ is in accordance with the calculations when the effective turbulence level of the wind tunnel facility is taken into account. However, calculations indicate for free flight conditions an extension of the low drag bucket to a lower lift coefficient. A detailed discussion about this phenomenon is given in Ref. 2 and 5.

Oil flow patterns, made at several angles of attack, show that the flow on the upper surface is on the verge of forming a laminar separation bubble. In the example of Fig. 12, transition is located at about 46% C.

The improvement of maximum lift coefficient is related to the reduction of separated flow, as shown in Fig. 13 and Fig. 14. Note the occurence in Fig. 14 of a laminar separation bubble on the nose of the upper half of the wing segment. A long laminar separation bubble is present on the lower surface, as shown in Fig. 15. Laminar separation occurs on the thin tape which covers the pneumatic turbulators (occasionally visible), and reattachment is just in front of the aileron slot (which is covered by tape for oil protection). A similar situation is present on the lower part in Fig. 16, while on the upper part the laminar separation bubble is shortened due to the disturbance of the blowing pneumatic turbulators. A further reduction in bubble length is

obtained by decreasing the interspace of the pneumatic turbulators, Fig. 17. Note the persistency of the bubble between the wedges originating from the blowing orifices.

The transition strip with bulges always eliminated the laminar separation bubble, as shown by the example of Fig. 18. Here the pneumatic turbulators have no clear effect on the bubble, however, traces of their activity are visible in the turbulent flow area behind. An increase of the air volume flow does cause turbulent wedges, Fig. 19, indicating that the peneumatic turbulators work like roughness with adjustable height.

Despite the rather long laminar separation bubble on the lower surface, both transition devices have only minor effect on the drag, contrary to the experimental results of the inner wing airfoil, Ref. 2. Because of the linear lofting between the inner wing airfoil and the tip airfoil, which have an abrupt beginning of the pressure-rise at 65% chord and 55% chord respectively, the pressure distribution of an intermediate airfoil is rounded in that area, thus forming some kind of instability region. Consequently, the laminar separation bubble is rather thin and no significant drag decrease can be obtained by using transition devices.

For the same reason, application of these transition devices on those existing airfoils which have instability regions will be ineffective or even harmful.

Fig. 20 shows the curves, for $Re = 0.85 * 10^6$ and several angles of aileron deflection, faired through a mass of data points and measured to study the wool tuft indicated separation problem in circling flight. At a typical lift coefficient of 1.2 and an angle of bank of 35 degrees, the aileron deflection needed to compensate for the spanwise variation in dynamic pressure is about 5 degrees. From Fig. 20 it is clear that the increase in lift for the downward deflected aileron is accompanied by a large increase in drag, due to flow separation in the aileron, Fig. 21. Since the upper surface of the tip airfoil was only slightly modified, this separation problem can be expected on every wing which has the well known FX60-126 airfoil in the tip. Several calculative attempts to postpone flow separation by modifying the upper surface between 60% C and 90% C (i.e., lowering the suction peak at the aileron hinge) had only limited success.

Development of a new tip airfoil seems justified. Maybe some kind of boundary layer control (blown flap) is needed to solve the problem.

Finally, the curious behavior of the drag curve for 10 degrees angle of airleron deflection below 1 degree angle of attack is related to the flow behavior on the upper surface. At decreasing angle of attack, transition moves rearward and is exactly on the hinge at $\alpha = -1.5^o$ where the drag is lowest. The pressure peak at the hinge, with steep pressure-rise thereafter (according to potential flow calculations), causes a thick laminar separation bubble at $\alpha < -1.5^o$ with accompanying drag increase.

REFERENCES

1. Boermans, L.M.M.; Selen, H.J.W; Wijnheijmer, M.L.: Wind tunnel Tests on Two Wing Segments of the ASW-19 Sailplane. Mem. M-379, Delft University of Technology, Dept. of Aerospace Engineering. August 1980.
2. Boermans, L.M.M.; Selen, H.J.W.: Design and Tests of Airfoils for Sailplanes with an Application to the ASW-19B. ICAS-82-5.5.2, August 1982.
3. Pfenninger, W.: Vergleich der Impulsmethode mit der Wagung bei Profilwiderstandsmessungen. Mitteilung 8 der ETH, Zurich, 1943.
4. Allen, H.J.; Vincenti, W.G.: Wall interference in a two-dimensional-flow wind tunnel, with consideration of the effect of compressibility. NACA report no. 782, 1944.
5. van Ingen, J.L.; Boermans, L.M.M.; Blom, J.J.H.: Low Speed Airfoil Section Research at Delft University of Technology. ICAS-80-10.1, October 1980.
6. Althaus, D.: Stuffgarter Profilkatalog I. Institut fur Aero- und Gasdynamik der Universitat Stuffgart. 1972.

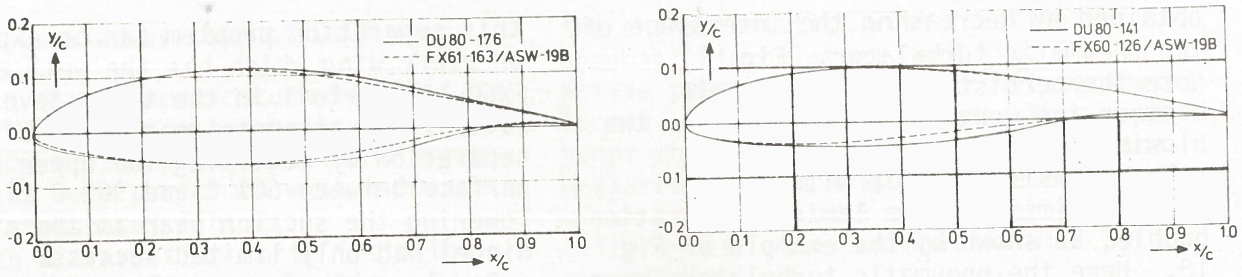

Fig. 3: New and original airfoils

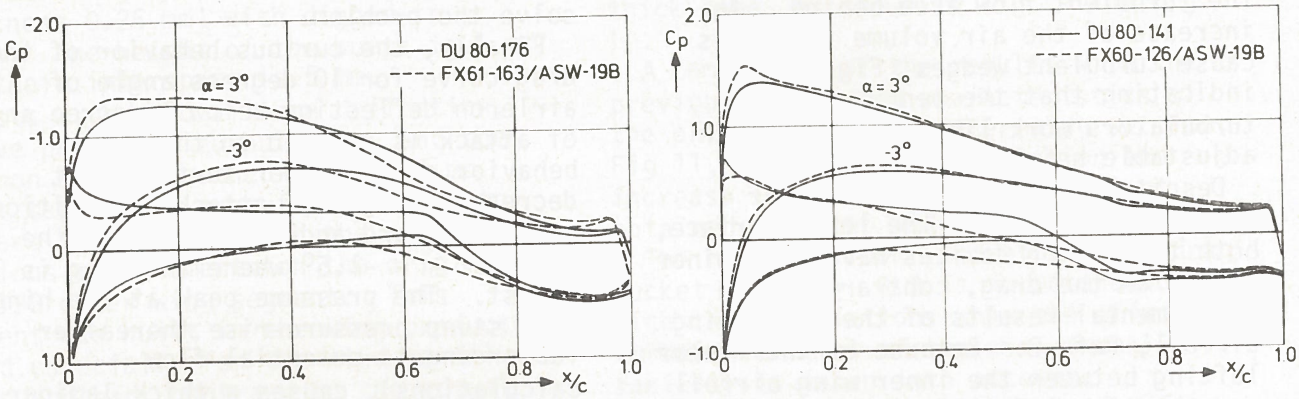

Fig. 4: Potential flow pressure distributions

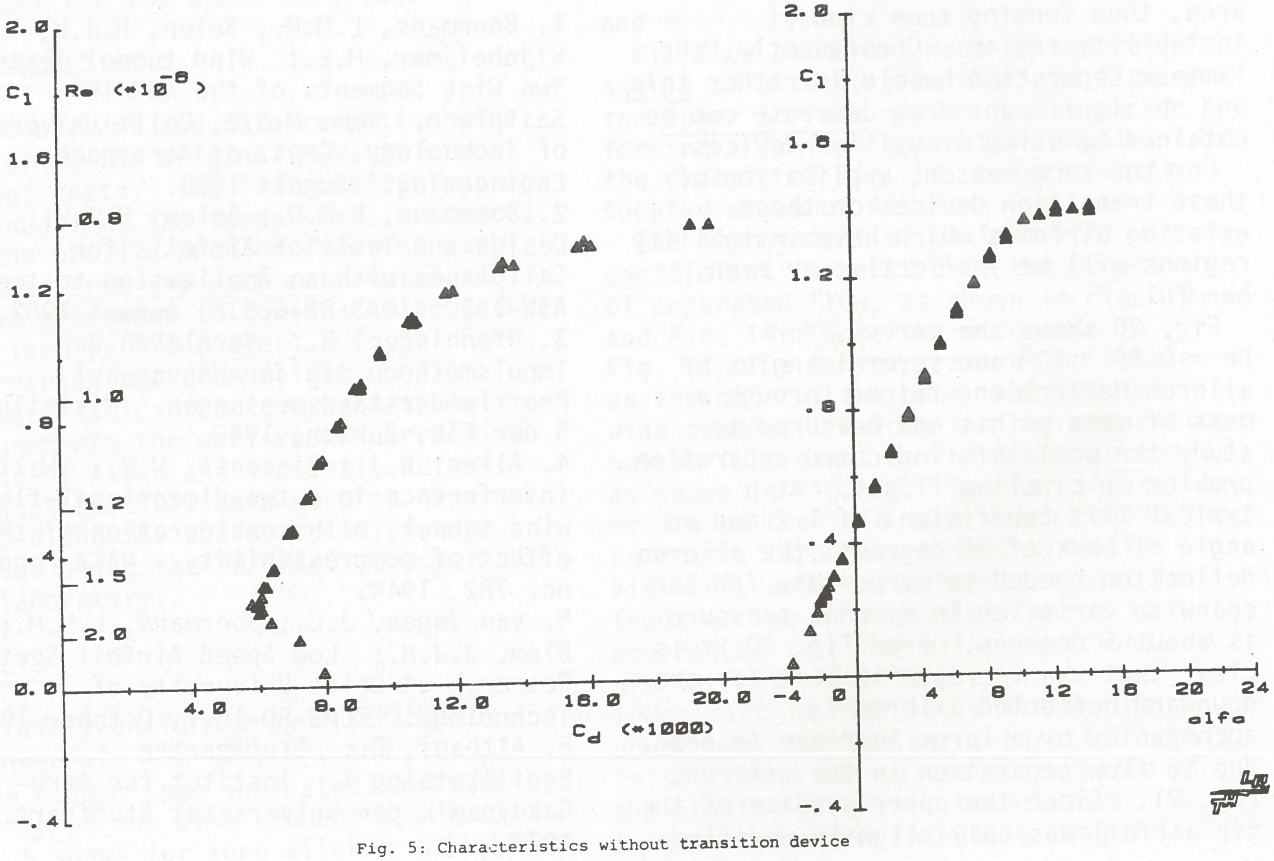

Fig. 5: Characteristics without transition device

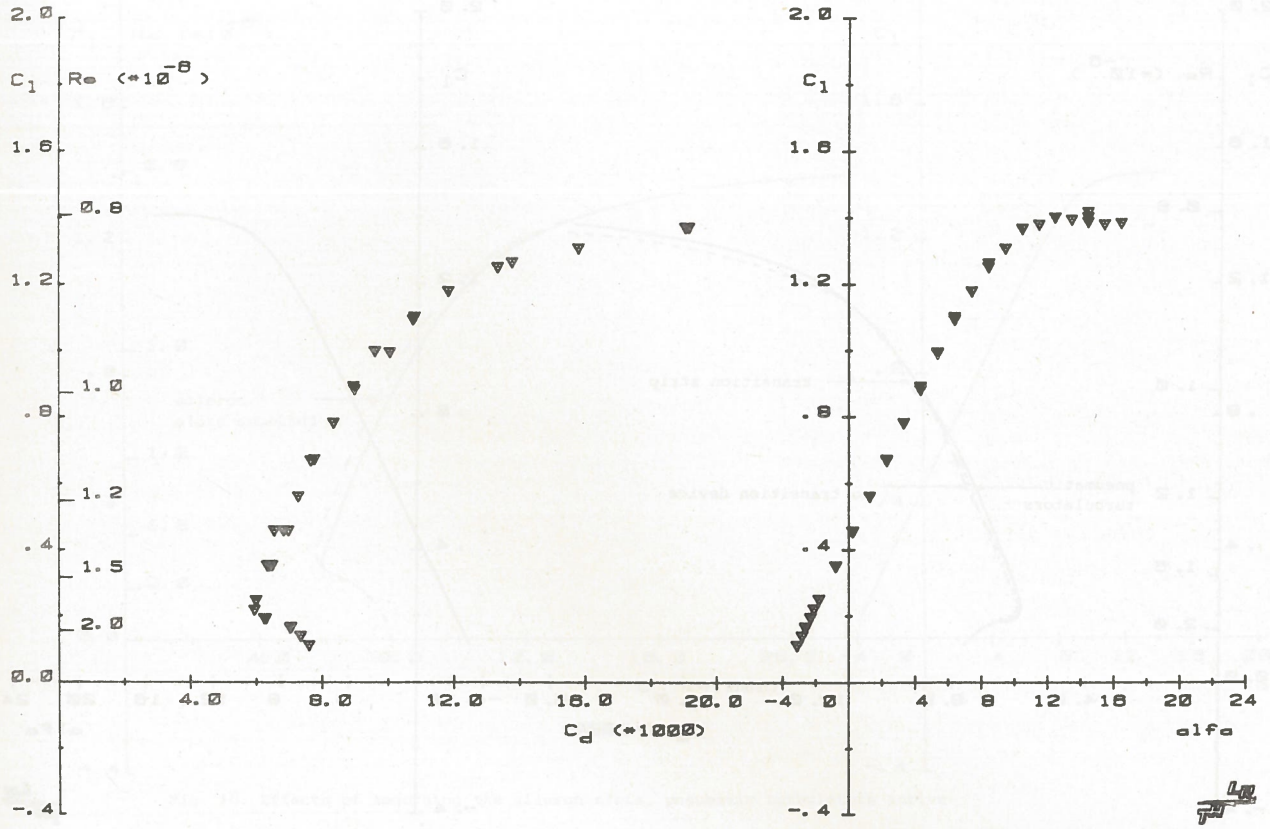

Fig. 6: Characteristics with pneumatic turbulators

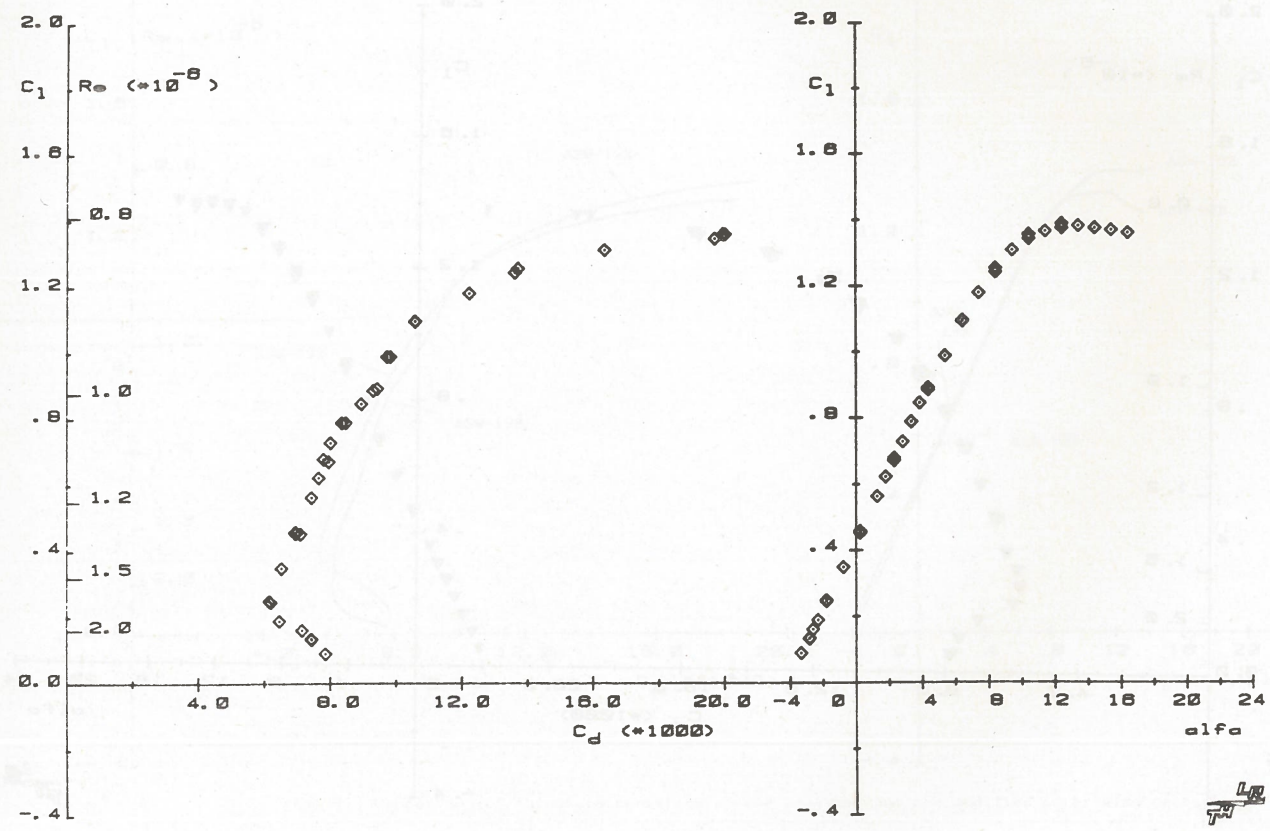

Fig. 7: Characteristics with transition strip

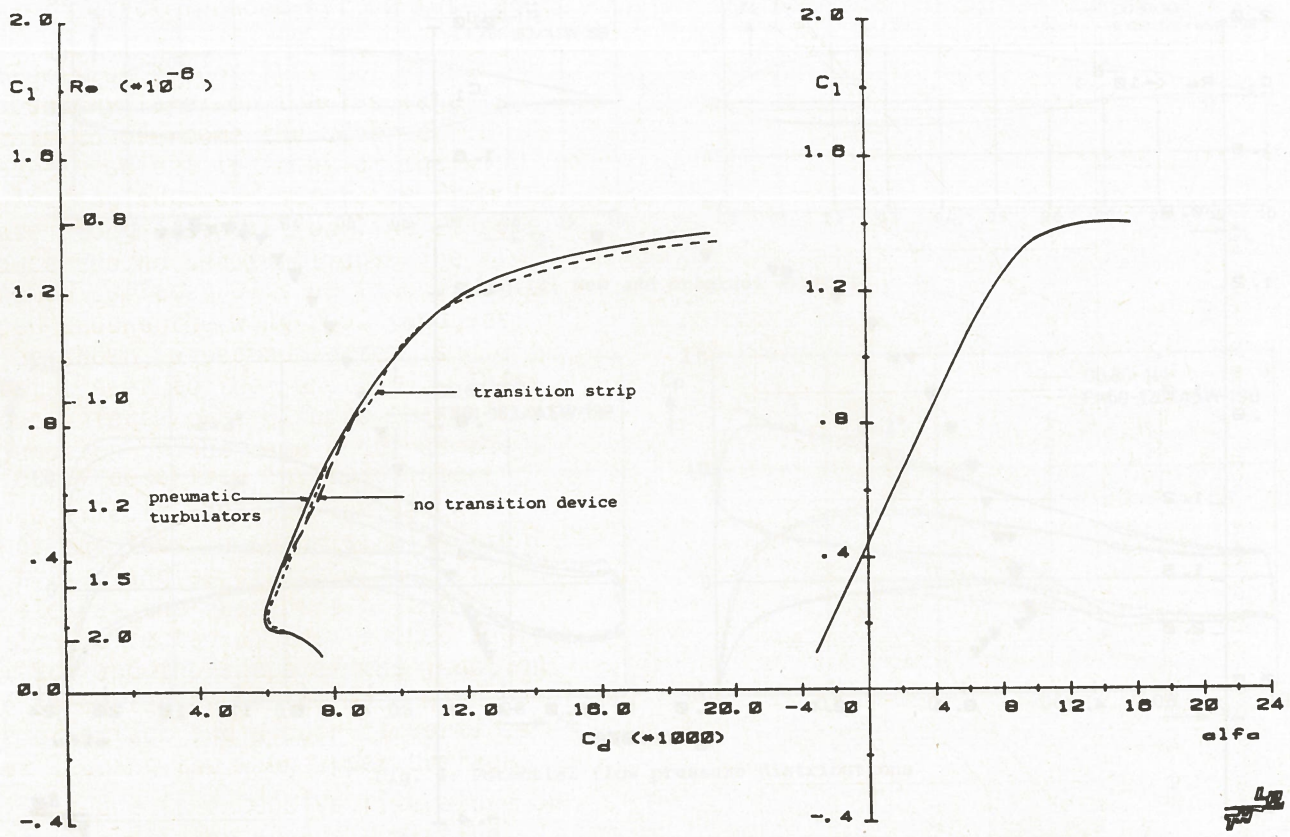

Fig. 8: Comparison of the characteristics with and without transition devices.

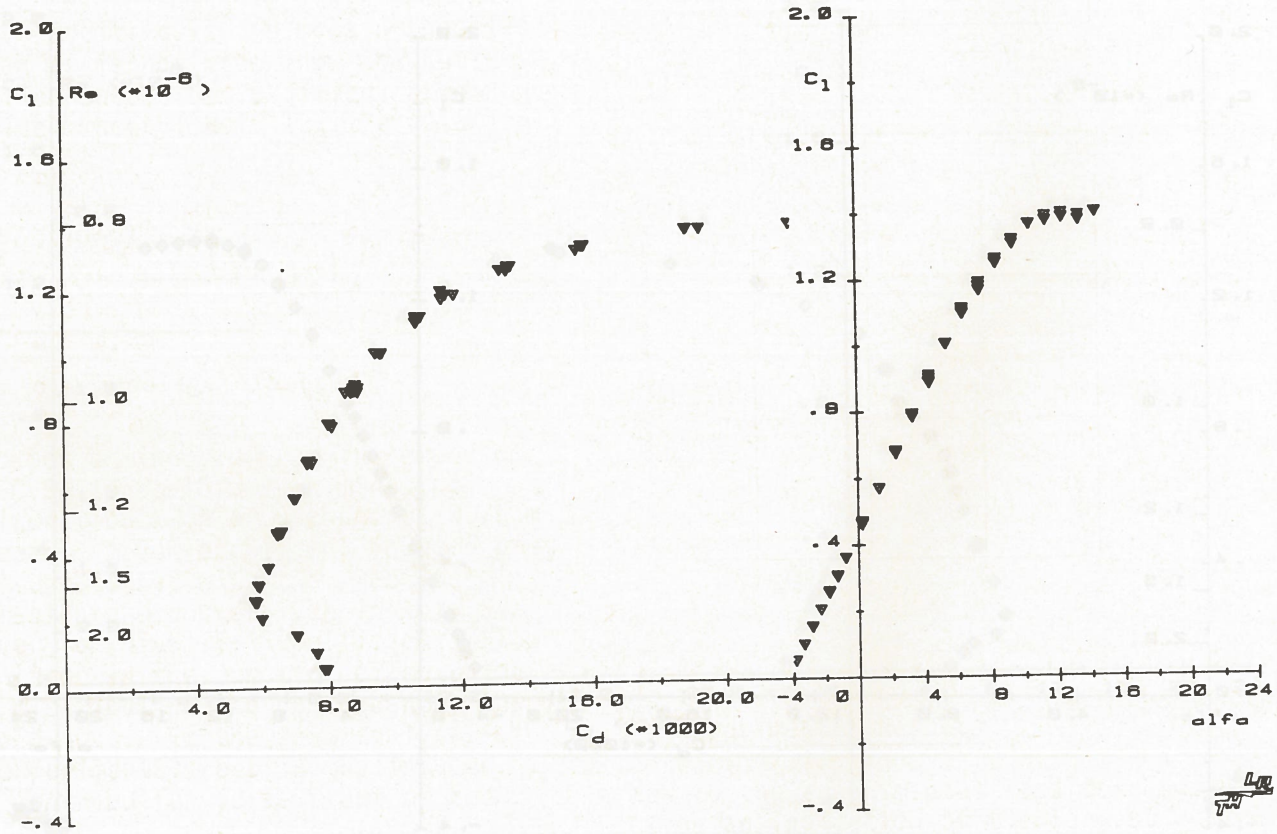

Fig. 9: Characteristics with the aileron slots smoothed, pneumatic turbulators active

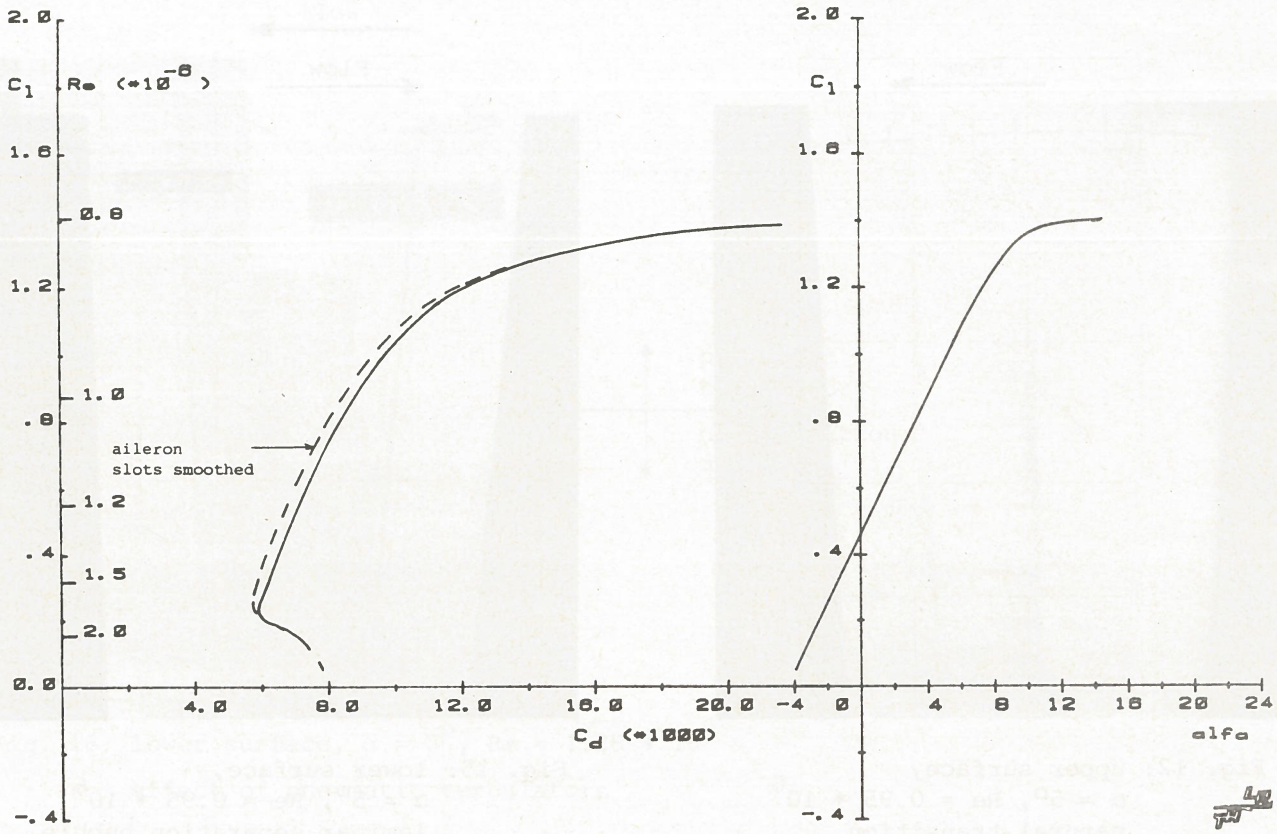

Fig. 10: Effects of smoothing the aileron slots, pneumatic turbulators active

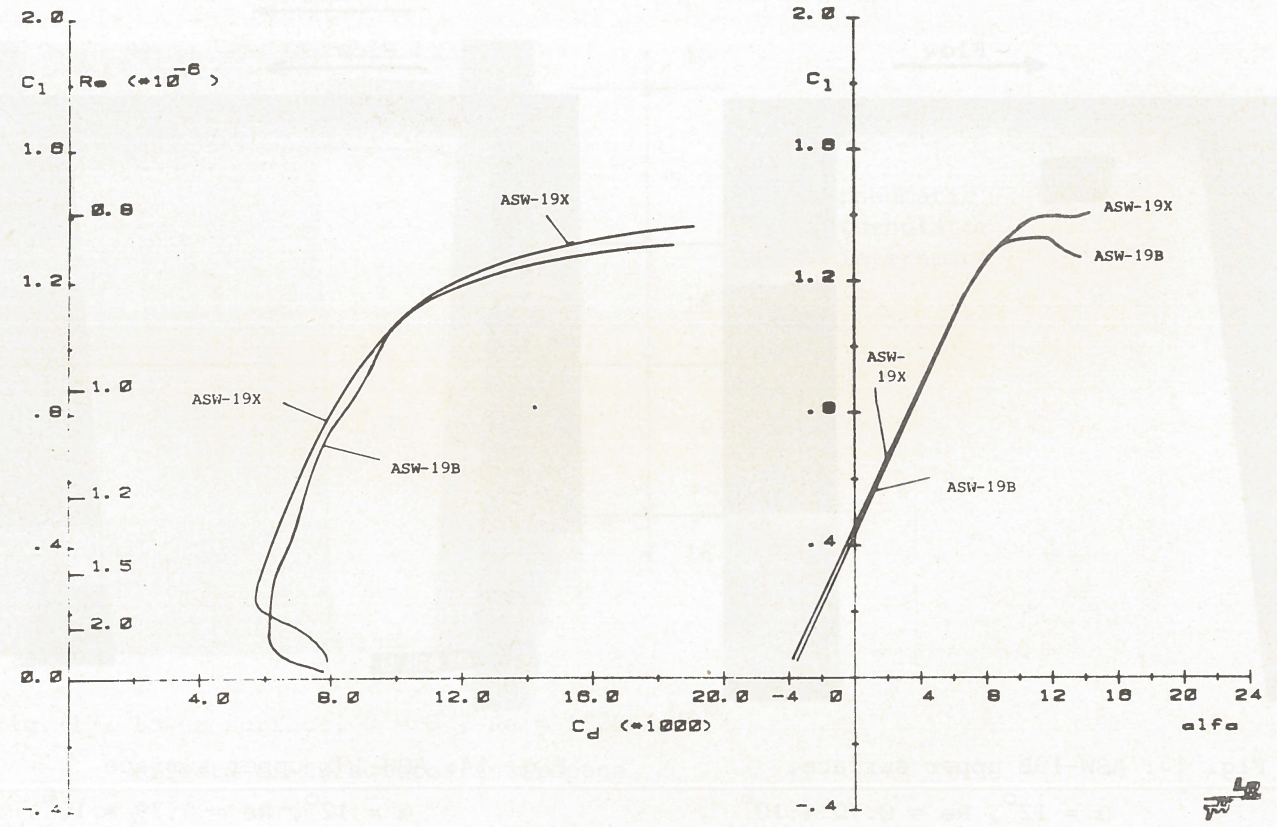

Fig. 11: Comparison of the characteristics of the original and the modified outer wing section

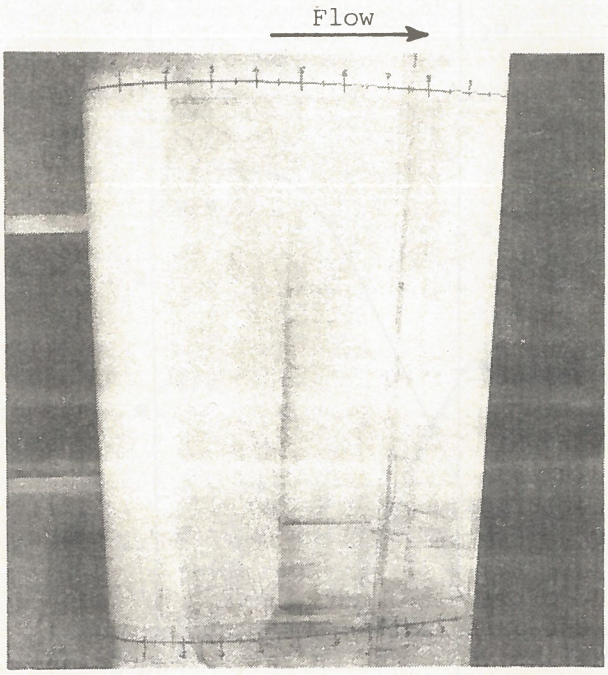

Fig. 12: upper surface,
$\alpha = 5^{o}$, Re = 0.95 * 10^{6}
natural transition

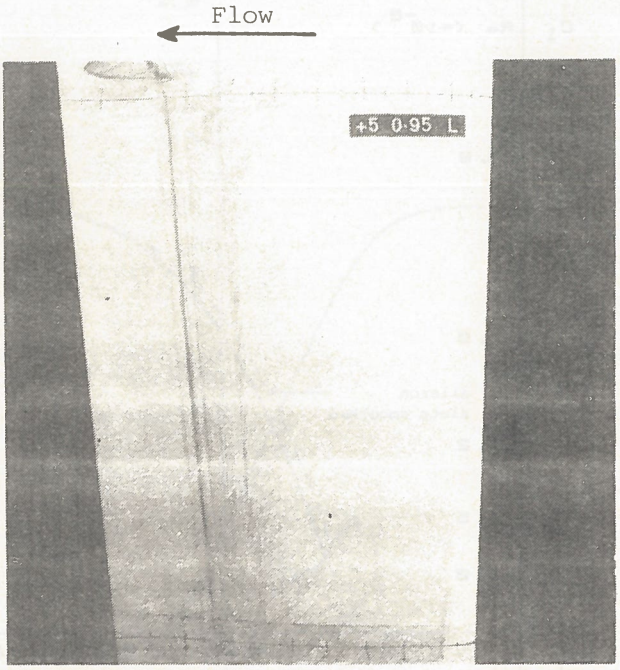

Fig. 15: lower surface,
$\alpha = 5^{o}$, Re = 0.95 * 10^{6}
laminar separation bubble

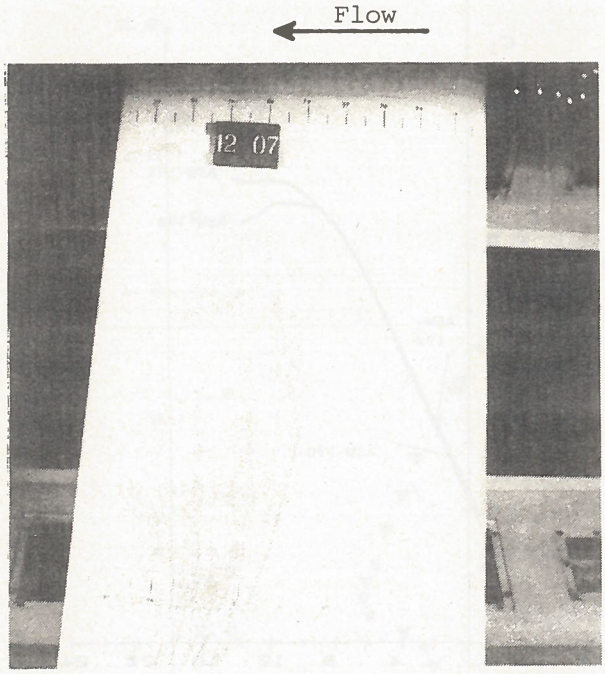

Fig. 13: ASW-19B upper surface,
$\alpha = 12^{o}$, Re = 0.70 * 10^{6}

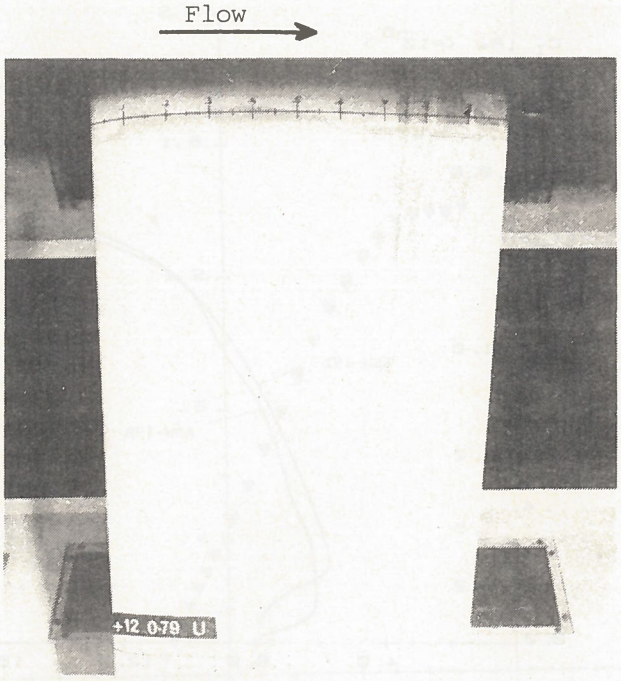

Fig. 14: ASW-19X upper surface
$\alpha = 12^{o}$, Re = 0.79 * 10^{6}

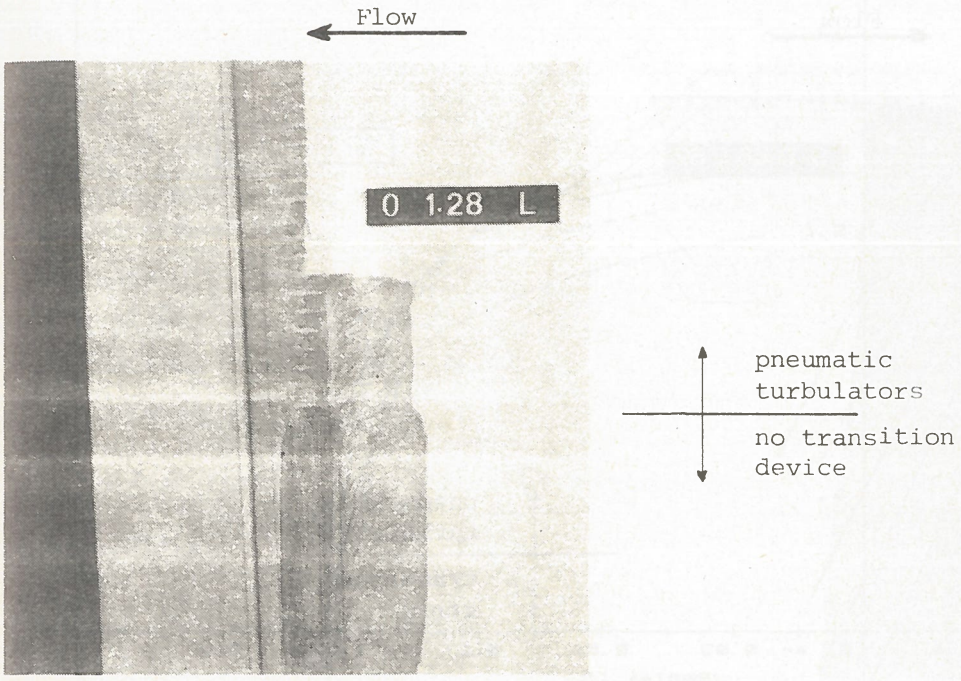

Fig. 16: lower surface, $\alpha = 0^{\circ}$, $Re = 1.28 * 10^{6}$
effect of pneumatic turbulators

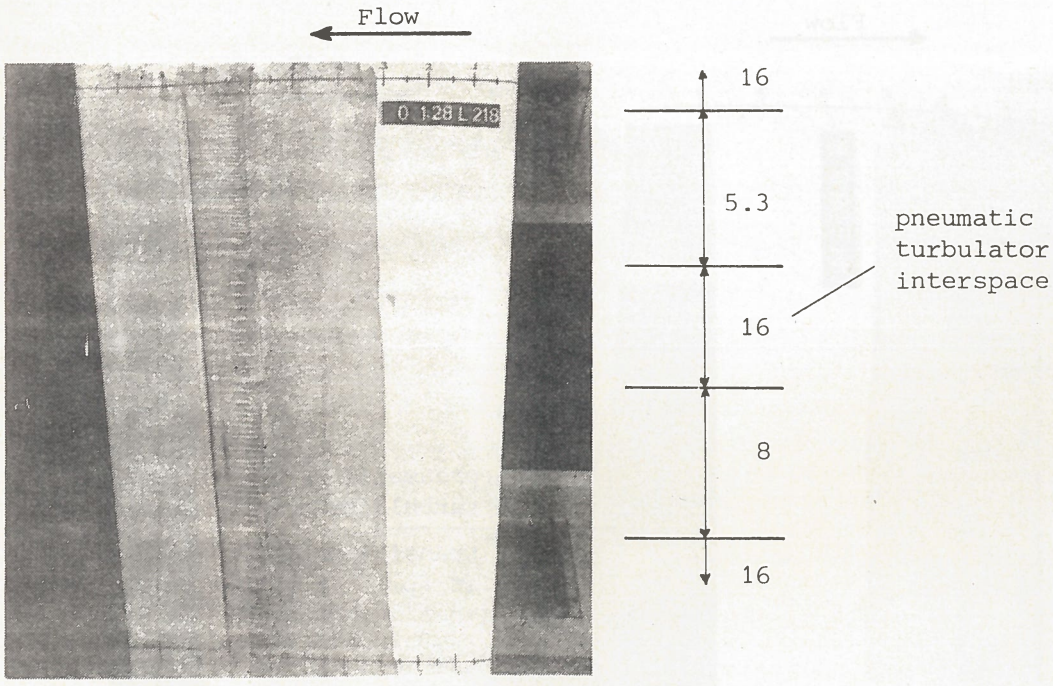

Fig. 17: lower surface, $\alpha = 0^{\circ}$, $Re = 1.28 * 10^{6}$
effects of turbulator interspace

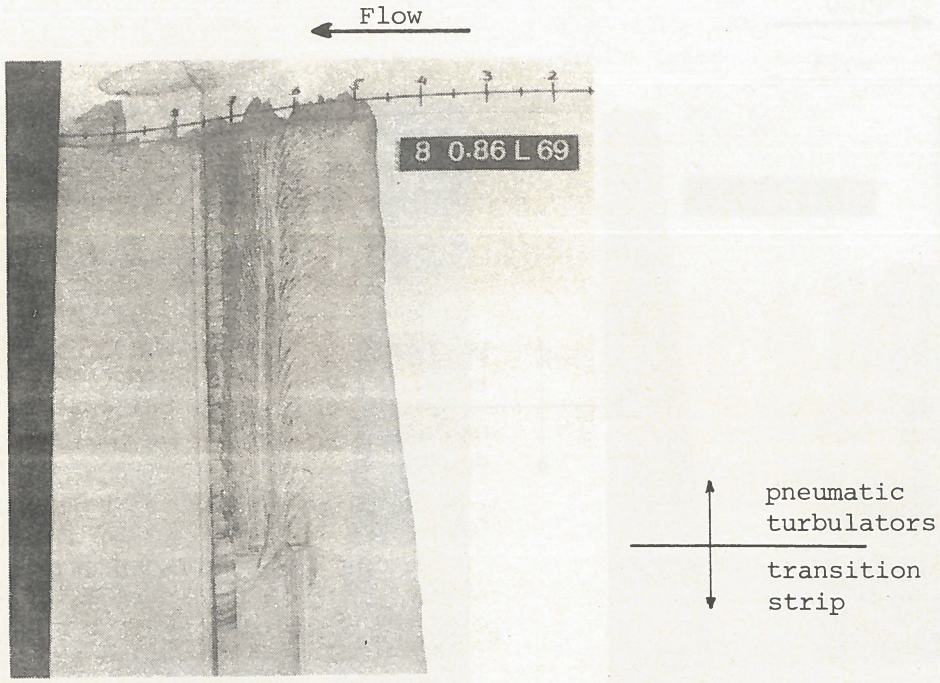

Fig. 18: lower surface, $\alpha = 8^{\circ}$, $Re = 0.86 * 10^{6}$

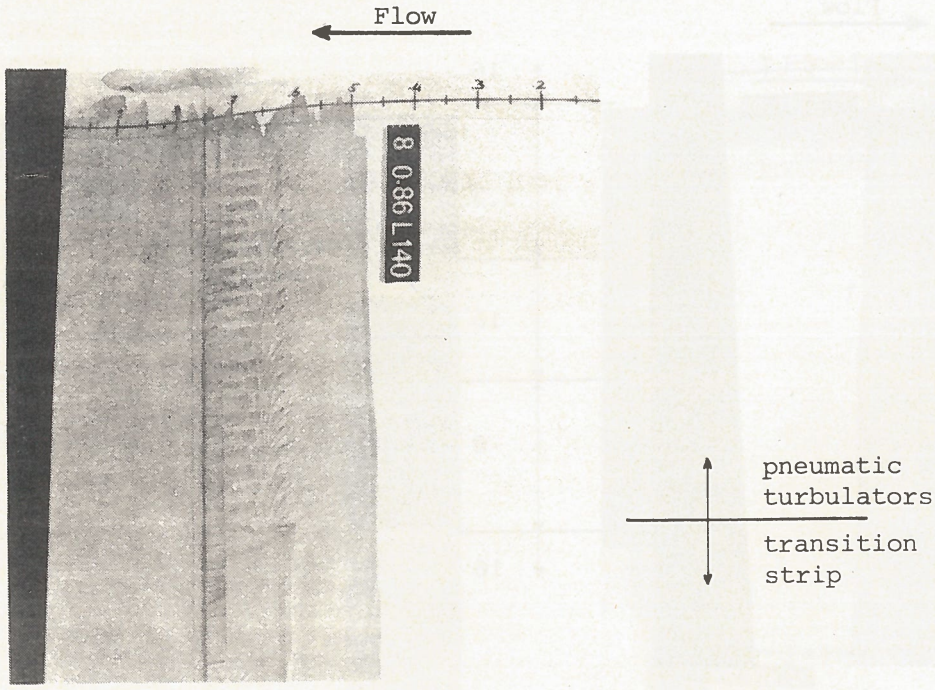

Fig. 19: lower surface, $\alpha = 8^{\circ}$, $Re = 0.86 * 10^{6}$

effect of doubling the air volume flow through the pneumatic turbulators

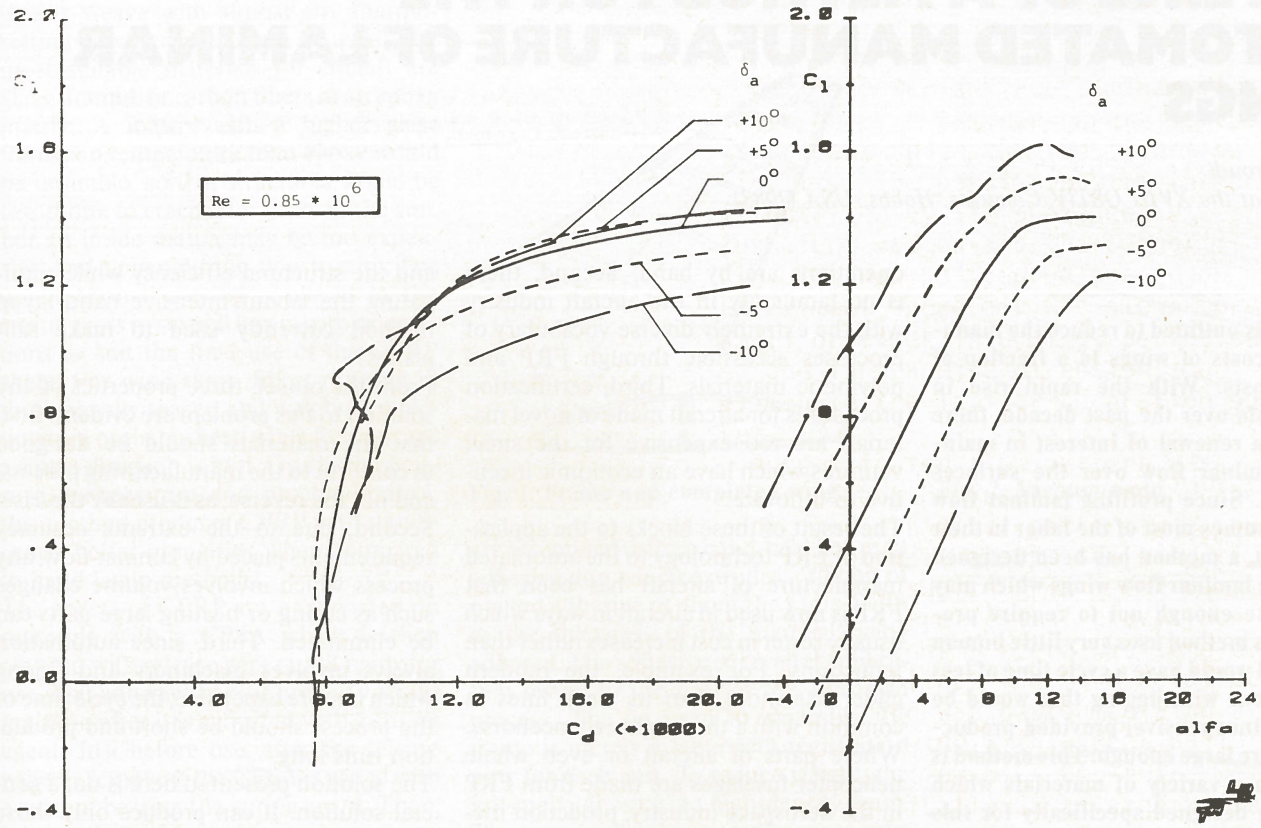

Fig. 20: Characteristics with aileron deflection (no transition device)

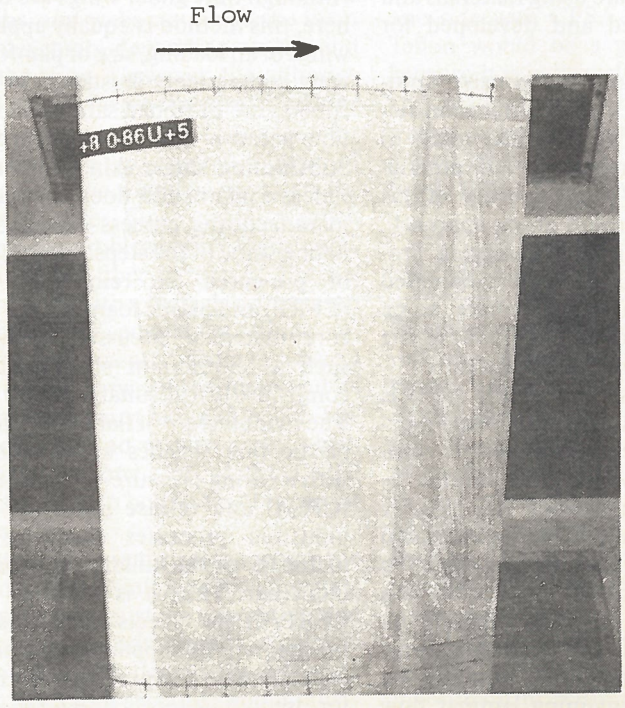

Fig. 21: upper surface, $\alpha = 8^{\circ}$, Re = $0.86 * 10^{6}$
separated flow on aileron deflected
+ 5 degrees